# The Influence of the Cylindrical Shape of the Nucleosomes and H1 Defects on Properties of Chromatin

Philipp M. Diesinger* and Dieter W. Heermann*†
*Department of Physics, Institut für Theoretische Physik, and †Interdisziplinäres Zentrum für Wissenschaftliches Rechnen, Heidelberg University, Heidelberg, Germany

ABSTRACT We present a model improving the two-angle model for interphase chromatin (E2A model). This model takes into account the cylindrical shape of the histone octamers, the H1 histones in front of the nucleosomes, and the distance *d* between the in and outgoing DNA strands orthogonal to the axis of the corresponding nucleosome cylinder. Factoring these chromatin features in, one gets essential changes in the chromatin phase diagram: Not only the shape of the excluded-volume borderline changes but also the orthogonal distance *d* has a dramatic influence on the forbidden area. Furthermore, we examined the influence of H1 defects on the properties of the chromatin fiber. Thus, we present two possible strategies for chromatin compaction: The use of very dense states in the phase diagram in the gaps in the excluded-volume, borderline, or missing H1 histones can lead to very compact fibers. The chromatin fiber might use both of these mechanisms to compact itself at least locally. Line densities computed within the model coincident with the experimental values.

## INTRODUCTION

The nucleosome is the basic repeat unit of chromatin (1) in all eukaryotic organisms. It consists of a cylindrical-shaped histone octamer and a stretch of DNA wrapped around the histone complex ~1.65 times. The histone octamer consists of four pairs of core histones (H2A, H2B, H3, and H4) and is known up to atomistic resolution (2,3). The nucleosomes are connected by naked DNA strands and together with these linkers, they form the so-called 30-nm fiber. The histone H1 (and the variant histone H5 with similar structure and functions) is involved in the packing of the beads on a string structure into the 30-nm chromatin structure. To do this, it sits in front of the nucleosome keeping the DNA in place; the DNA is wrapped around the histone octamer, and thus stabilizes the chromatin fiber. H1 depletion can cause dramatic alterations in the chromatin structure (4).

The nucleosome provides the lowest level of compaction and, furthermore, it is important in the regulation of transcription. Several enzymes can change the position of the nucleosome (5) to make the genetic information, held within the nucleosome-core particle, accessible.

The compaction of the DNA plays a very important role in modern biophysics since it has a total length of some meters but has to fit into a nucleus of some microns. The degree of compaction depends on the salt concentration (6) and on the presence of linker histones (7). The presence of the linker histones leads to the formation of stemlike structures that are formed by the incoming and outgoing DNA string in front of the nucleosome. In vitro experiments show that, at low salt concentration, a 10-nm structure is formed with a string-of-beads shape (6). At high salt concentrations, the chromatin fiber is much more compact, and has a diameter of 30 nm (8).

The chromatin structure is still not completely understood (1,9–11). There are different models for its structure: zigzag ribbon models (7,12–15); helical solenoid models (6,16,17); coarse-grained models on a larger scale (18); or no regular structure at all (10). A crystal structure of a tetranucleosome has been revealed (12) and used to construct a model for the 30-nm fiber resembling a zigzag ribbon that twists or supercoils. The chromatin fiber has been investigated by electron cryo-microscopy (7,19), atomic force microscopy (20,21), and neutron scattering and scanning transmission electron microscopy (22). Beyond the 30-nm level, chromatin is poorly understood.

The two-angle model was introduced by Woodcock et al. (13) to describe the geometry of the 30-nm chromatin fiber. It has been shown that the excluded volume of the histone complex plays a very important role for the stiffness of the chromatin fiber (23) and for the topological constraints during condensation/decondensation processes (24). In Schiessel (25), a rough approximation of the forbidden surface in the chromatin phase diagram was given. In a previous work of ours (26), we answered questions concerning the fine structure of the excluded volume borderline separating the allowed and forbidden states in the phase diagram with the basic assumption of spherical nucleosomes and no-orthogonal-shift between the in and outgoing strands. Here we present a Ramachandran-like diagram for chromatin fibers with cylindrical nucleosomes for a new extended model and furthermore discuss the influence of an orthogonal shift between the linkers due to H1 histones and the volume exclusion of the DNA.

We first present the basic notations for the formulation of the extended two-angle model (E2A). Then we give an algorithm for the generation of chains within the model and

*Submitted June 1, 2007, and accepted for publication October 22, 2007.*

Address reprint requests to Philipp M. Diesinger, Tel.: 49-6221-54-9449; E-mail: diesinger@tphys.uni-heidelberg.de.

Editor: Stuart M. Lindsay.


0006-3495/08/06/4165/08 $2.00

doi: 10.1529/biophysj.107.113902

present the resulting phase diagram and end-to-end distance as well as radius of gyration results.

## THEORY

### Extended two-angle model

We extend the two-angle model by introducing a parameter for the orthogonal distance between the DNA strands in front of the nucleosome. Furthermore, we take the cylindrical excluded volume of the nucleosomes into account as well as the H1 histones that fix the DNA linkers in front of the nucleosome. The H1 histones themselves are taken to be random variables to allow for possible missing H1 histones.

### Basic notations

We start out and fix some basic notations to use for the formulation of the model. The nucleosomes will be characterized by the centers $N_i \in \mathcal{R}^3$ and the orientations $\hat{p}_i \in \mathcal{R}^3$ of the nucleosomes, with $i = 0, \ldots, N$ and $\| \hat{p}_i \| = 1$. $N$ is the length of the fiber. The linkers between the centers of two nucleosomes will be denoted by $b_i = N_i - N_{i-1}$ with $i = 1, \ldots, N$. The length $\|b_i\|$ of the linkers will be a further input parameter of the model (opposite of the direction $b_i \in \mathcal{R}^3$ of the linkers). Furthermore, the entry-exit angle $\alpha_i \in [0, \pi]$ between two consecutive linkers is defined by $\alpha_i = \sphericalangle(-b_i, b_{i+1})$ with $i = 1, \ldots, N-1$ and the rotational angle $\beta_i \in [0, \pi]$ between two consecutive orientations is given by $\beta_i = \sphericalangle(p_{i-1}, p_i)$ with $i = 1, \ldots, N$.

Moreover, $h_i$ represents the distance along the orientational axis $\hat{p}_{i-1}$ from $N_{i-1}$ to $N_i$ due to the spatial discrepancy between the in and outgoing DNA strands. The value $h_i$ can be expressed by the orthogonal distances $d_i$ that the DNA covers by wrapping itself around the histone complexes: $h_i = \frac{1}{2}(d_{i-1} + d_i)$ with $i = 1, \ldots, N$.

Thus, a single chromatin strand within the two-angle model is characterized by the following set of variables:

$$(\{\alpha_i\} i \in \{1,..,N-1\}, \{\beta_i\} i \in \{1,..,N\},$$
$$\{h_i\} i \in \{1,..,N\}, \{\|b_i\|\} i \in \{1,..,N\}).$$

The general rotational matrix $\mathcal{R}$ around an axis $\hat{a} = (a_1, a_2, a_3)^t$ (with $\| \hat{a} \| = 1$) by an angle $\gamma$ with respect to the right-hand rule will be used in the following. It is given by

$$\mathcal{R}_{\hat{a}}^{\gamma} = \begin{pmatrix} \cos\gamma + a_1^2(1-\cos\gamma) & a_1a_2(1-\cos\gamma) - a_3\sin\gamma & a_1a_3(1-\cos\gamma) + a_2\sin\gamma \\ a_2a_1(1-\cos\gamma) + a_3\sin\gamma & \cos\gamma + v_2^2(1-\cos\gamma) & a_2a_3(1-\cos\gamma) - a_1\sin\gamma \\ a_3a_1(1-\cos\gamma) - a_2\sin\gamma & a_3a_2(1-\cos\gamma) + a_1\sin\gamma & \cos\gamma + a_3^2(1-\cos\gamma) \end{pmatrix}.$$

### Definition of the two-angle model

A chromatin fiber within the framework of the extended two-angle model has to fulfill the following conditions for all $i \in \{1, \ldots, N\}$:

Condition 1: $\sphericalangle(-b_i, b_{i+1}) = \alpha_i \Leftrightarrow \cos(\alpha_i) = \dfrac{\langle -b_i, b_{i+1} \rangle}{\|b_i\| \|b_{i+1}\|}$.

Condition 2: $\sphericalangle(\hat{p}_{i-1}, \hat{p}_i) = \beta_i \Leftrightarrow \cos(\beta_i) = \langle \hat{p}_{i-1}, \hat{p}_i \rangle$.

Condition 3: $\| N_i - N_{i-1} \| = \|b_i\|$.

Condition 4: $\langle \hat{p}_{i-1}, b_i \rangle \hat{p}_{i-1} = h_i = \dfrac{1}{2}(d_{i-1} + d_i)$.

These are illustrated in Fig. 1.

The first condition adjusts the entry-exit angle of nucleosome $i$ to the given parameter $\alpha_i$. The second condition does the same for the rotational angle due to the DNA twist from nucleosome $i-1$ to nucleosome $i$. The third condition fixes the distance of the two consecutive nucleosomes $i-1$ and $i$ and the last condition adjusts the orthogonal distance along the local chromatin axis between the nucleosomes $i-1$ and $i$.

### Construction of the fiber

The construction of the fiber can be done using an iterative process. A further part of the model is the presence of a H1 histone that is assumed to be present with probability $p$.

The first nucleosome center and its orientation are arbitrary. We chose

$$N_0 = \begin{pmatrix} 0 \\ 0 \\ 0 \end{pmatrix}, \quad \hat{p}_0 = \begin{pmatrix} 0 \\ 0 \\ 1 \end{pmatrix}.$$

The following vectors fulfill the conditions of the two-angle model for the second nucleosome location and its orientation,

$$N_1 = N_0 + \sqrt{\| b_1 \|^2 - h_1^2} \begin{pmatrix} -1 \\ 0 \\ 0 \end{pmatrix} + h_1 \hat{p}_0 = \begin{pmatrix} -\sqrt{\| b_1 \|^2 - h_1^2} \\ 0 \\ h_1 \end{pmatrix}$$

and

$$\hat{p}_1 = \mathcal{R}_{\hat{a}}^{\beta_1} \hat{p}_{i-1} \quad \text{with} \quad \hat{a} = (1,0,0)^t.$$

Now we can calculate $N_{i+1}$ and $\hat{p}_{i+1}$ in dependence of $N_i$, $N_{i-1}$, $\hat{p}_i$, and $\hat{p}_{i-1}$. With

$$v_i := -b_i + \langle \hat{p}_i, -b_i \rangle \hat{p}_i$$

and

$$v_i' := \mathcal{R}_{\hat{p}_i}^{\alpha_0} \sqrt{b_{i+1}^2 - d_{i+1}^2} \left( \frac{v_i}{\|v_i\|} \right) + h_{i+1} \hat{p}_i, \qquad (1)$$

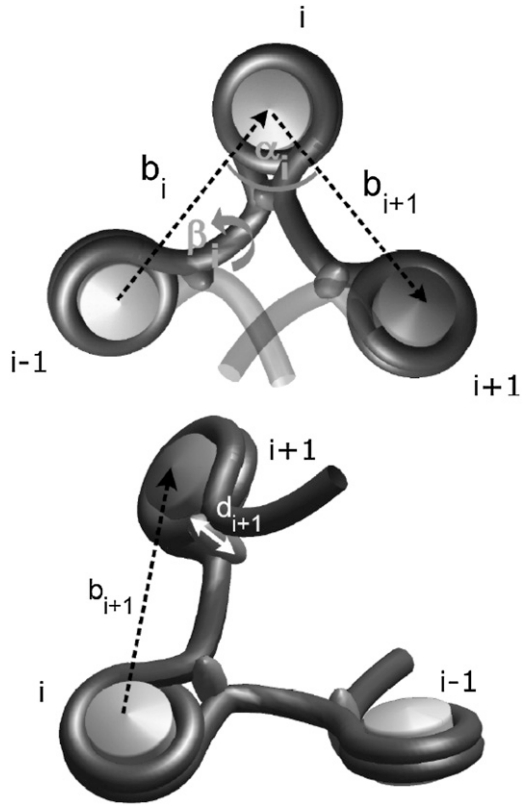


FIGURE 1 The figure shows the basic parameters of the E2A model: the entry-exit angle $\alpha_i$, the rotational angle $\beta_i$, the linker length $b_i$, and the orthogonal distance $d_i$ between the in and outgoing linkers. We chose a large entry-exit angle here to make the visualization clear.

one gets the location of nucleosome $i + 1$ by

$$N_{i+1} = N_i + v_i'.$$

The value $\alpha_0$ is the angle between the projections of $b_{i+1}$ and $-b_{i-1}$ onto an arbitrary plane orthogonal to $\hat{p}_i$. We need to calculate the dependence of this projected entry-exit angle $\alpha_0$ on the actual entry-exit angle $\alpha$.

Note that $\alpha_0$ was used as entry-exit angle in some other publications (14,25) but in this work, it denotes only the projection of the real entry-exit angle $\alpha$.

Using the law of cosine one gets

$$l^2 = b_i^2 + b_{i+1}^2 - 2b_i b_{i+1}\cos(\alpha). \quad (2)$$

Now we will use an affine transformation $T$ to a new coordinate system $(x, y, z) \xrightarrow{T} (x', y', z')$ to get a second relation for $l$. We shift the origin to $N_i$ and rotate our old coordinate system so that $\hat{p}_i$ corresponds to the new $z$ axis. Furthermore, the new $x$ axis has to coincide with the projection of $-b_i$ onto any plane orthogonal to $\hat{p}_i$. Obviously,

$$l^2 = \|b_i + v_i'\|^2 = \|b_i' + v_i''\|^2$$

with

$$b_i \xrightarrow{T} b_i' = \begin{pmatrix} \sqrt{b_i^2 - \langle \hat{p}_i, -b_i\rangle^2} \\ 0 \\ \langle \hat{p}_i, -b_i\rangle \end{pmatrix},$$

and

$$v_i' \xrightarrow{T} v_i'' = \begin{pmatrix} \cos(\alpha_0)\sqrt{b_{i+1}^2 - h_{i+1}^2} \\ \sqrt{b_{i+1}^2 - h_{i+1}^2 - \left(\cos(\alpha_0)\sqrt{b_{i+1}^2 - h_{i+1}^2}\right)^2} \\ h_{i+1} \end{pmatrix}.$$

This leads to

$$l^2 = b_{i+1}^2 + b_i^2 - 2h_{i+1}\langle \hat{p}_i, -b_i\rangle - 2\cos(\alpha_0)\sqrt{b_i^2 - \langle \hat{p}_i, -b_i\rangle^2}\sqrt{b_{i+1}^2 - h_{i+1}^2}. \quad (3)$$

By comparing Eqs. 2 and 3, one gets eventually

$$\cos(\alpha_0) = \frac{b_i b_{i+1}\cos(\alpha) - h_{i+1}\langle \hat{p}_i, -b_i\rangle}{\sqrt{b_{i+1}^2 - h_{i+1}^2}\sqrt{b_i^2 - \langle \hat{p}_i, -b_i\rangle^2}},$$

with the boundary condition

$$\alpha_0 > \alpha_{\min} = \operatorname{acos}\left(\frac{(h_{i+1} + \|\langle \hat{p}_i, b_i\rangle\|)^2 - b_{i+1}^2 - b_i^2}{-2b_i b_{i+1}}\right), \quad (4)$$

due to nonvanishing $d_i$ and $d_{i+1}$. The calculation of $N_{i+1}$ is complete, since we now know the dependence of $\alpha_0$ on $\alpha$ and therefore one can use Eq. 1 to determine $N_{i+1}$. But one still has to calculate the orientation $p_{i+1}$ of nucleosome $N_{i+1}$. Due to the fixation of the in and outgoing DNA strand by the H1 histones, this orientation can be calculated by a rotation around the following normalized axis $\hat{a}$:

$$\hat{a} := \frac{-b_{i+1} - \langle p_i, -b_{i+1}\rangle \hat{p}_i}{\|\hat{a}\|}.$$

$\hat{p}_{i+1}$ then follows by a rotation of $\hat{p}_i$ around the axis

$$\hat{p}_{i+1} = \mathcal{R}_{\hat{a}}^{\beta_{i+1}} \hat{p}_i.$$

## METHODS

### Chromatin phase diagram

First, we determine the influence of the cylindrical excluded volume of the nucleosomes and a nonvanishing orthogonal distance between the in and outgoing DNA strands on the phase diagram of chromatin. Both of these parameters have been neglected so far (25,26). To determine this influence, we made simulations (27) of regular chromatin fibers and checked whether they fulfill the excluded volume conditions or not. We were able to plot our results in a Ramachandran-like diagram (see Fig. 3) and thus find out which states of the whole phase diagram are forbidden by excluded volume interactions and which are not. The fibers we simulated for this part were regular, i.e., all linker lengths, entry-exit angles, rotational angles, and $h_i$ were fixed for a certain strand.

The cylinders had a height of 16.8 ⟨bp⟩ and a diameter of 33.0 ⟨bp⟩, according to Wolffe (28). They were oriented by using the vectors $p_i$ above. Moreover, we assumed a DNA diameter of 6.6 ⟨bp⟩, a twist length of 10.2

⟨bp⟩, a mean linker length of 63 ⟨bp⟩, and that 1.65 turns of DNA are wrapped around the histone octamers.

### Fibers with H1 defects

Furthermore, we made Monte Carlo simulations of chromatin fibers with H1 defects; i.e., some of the H1 histones were missing. We used the two-angle model with some fixed parameters (see above), which reflects the probable mean values within the cell. The only interaction potential is the hard-core excluded volume. In this mean-field-like approach we neglect (29) thermal fluctuations to concentrate on the interaction between H1 defects and volume exclusion.

For a certain nucleosome $N_i$, the defect probability $p$ gives the chance of a missing H1 histone. If the histone is missing, the in and outgoing DNA strands are no longer fixed in front of the nucleosome but instead are arbitrary with respect to the excluded volume interactions of the chromatin strand (Fig. 2). Thus, we get results for the mean end-to-end distance and the mean radius of gyration of fibers with various defect probabilities: $p = 0.00$, $p = 0.01$, $p = 0.05$, $p = 0.10$, and $p = 0.30$. For these simulations we fixed the entry-exit angles $\alpha_i$ to 40°, the rotational angles $\beta_i$ to 36° and $h_i = 7$ ⟨bp⟩.

## RESULTS

### Phase diagram

The colored lines in Fig. 3 represent the phase transition between allowed and forbidden states. All states below the corresponding line are forbidden; those above it are allowed. The states near the excluded volume borderline are the most interesting of the phase diagram since they are the most compact ones (Fig. 4). Therefore, the gaps in the borderline might be used by the fiber to become (at least locally) very dense.

There is another borderline at the left side of the diagram that prevents $\alpha$ from getting smaller than some minimal value $\alpha_{min}(h)$, which depends on $h$. (This arrowlike structure can be seen best in Fig. 6.) It shifts toward larger $\alpha_{min}(h)$ with increasing $d$. The gap in this line is a further consequence of the cylindrical excluded volume and cannot be seen in the phase diagram for spherical nucleosomes (26). Fibers with a small entry-exit angle $\alpha$ and $\beta \ll \pi$ resemble zig-zag structures.

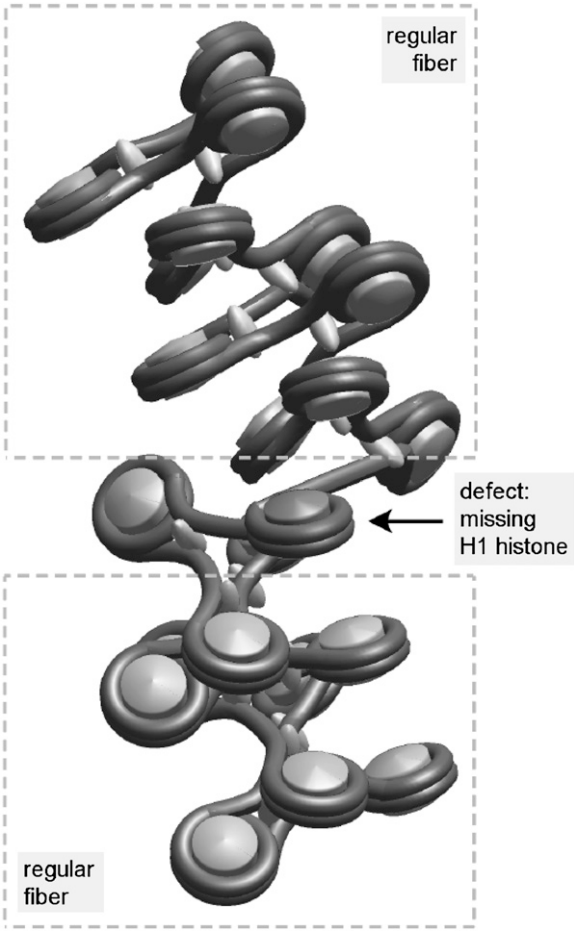


FIGURE 2 Shown is an example of a H1 defect within the chromatin fiber. The upper strand and the strand below the defect are regular.

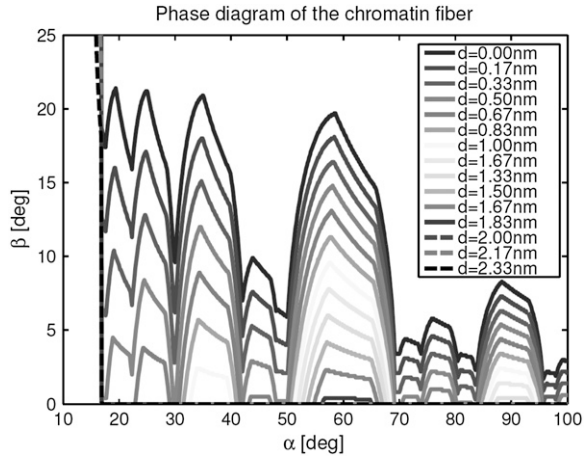


FIGURE 3 Cutout of the chromatin phase diagram (for different $d$). The states below the corresponding lines are forbidden due to excluded volume interactions. With increasing $d$, more and more states become accessible to the fiber.

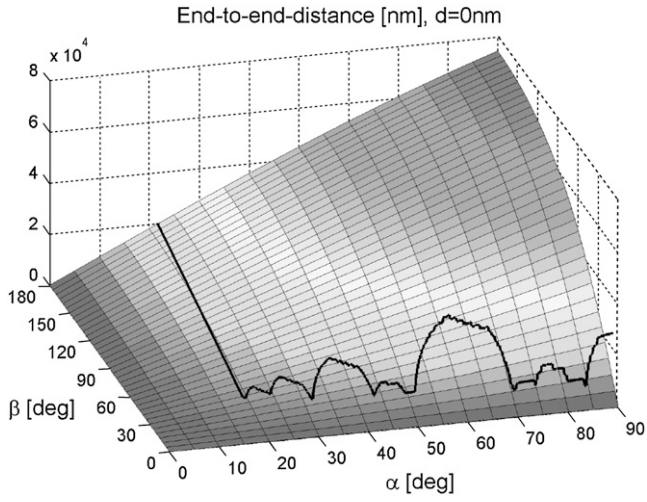


FIGURE 4 The end-to-end distance of regular chromatin fibers along a cutout of the phase diagram with fixed fiber length ($N = 500$ segments) and fixed $d = 0.0$ ⟨bp⟩. The solid black line represents the corresponding phase transition.

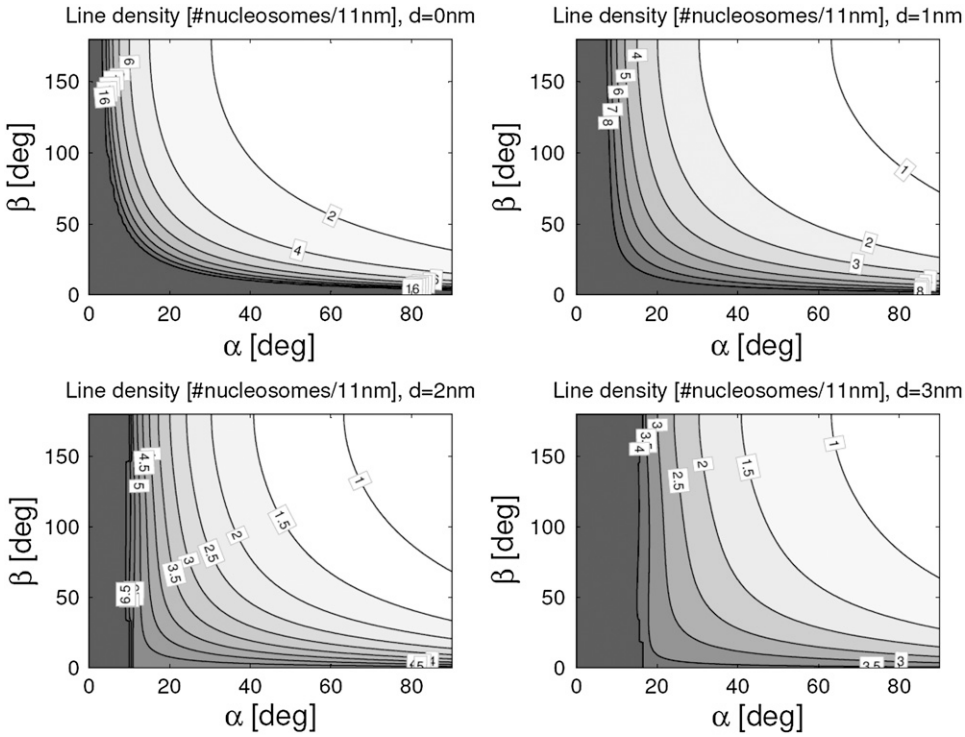


FIGURE 5 The line density of the nucleosomes within a regular chromatin fiber is large for small $\beta_i$. However, the comparison with the phase diagram shows that some of these states are forbidden due to excluded volume interactions.

Those with large entry-exit angles and $\beta \approx \pi$ look like solenoids. A comprehensive discussion of the different structures of the phase diagram can be found in the literature (25,26). Here we address only the changes due to cylindrical (instead of spherical) excluded volume.

As a consequence of the cylindrical instead of spherical excluded volume of the nucleosomes, the shape of the peaks in the phase diagram is changed: Their top shows a wedgelike shape due to the edges of the cylinders. With increasing entry-exit angle $\alpha$ there is more space between the nucleo-

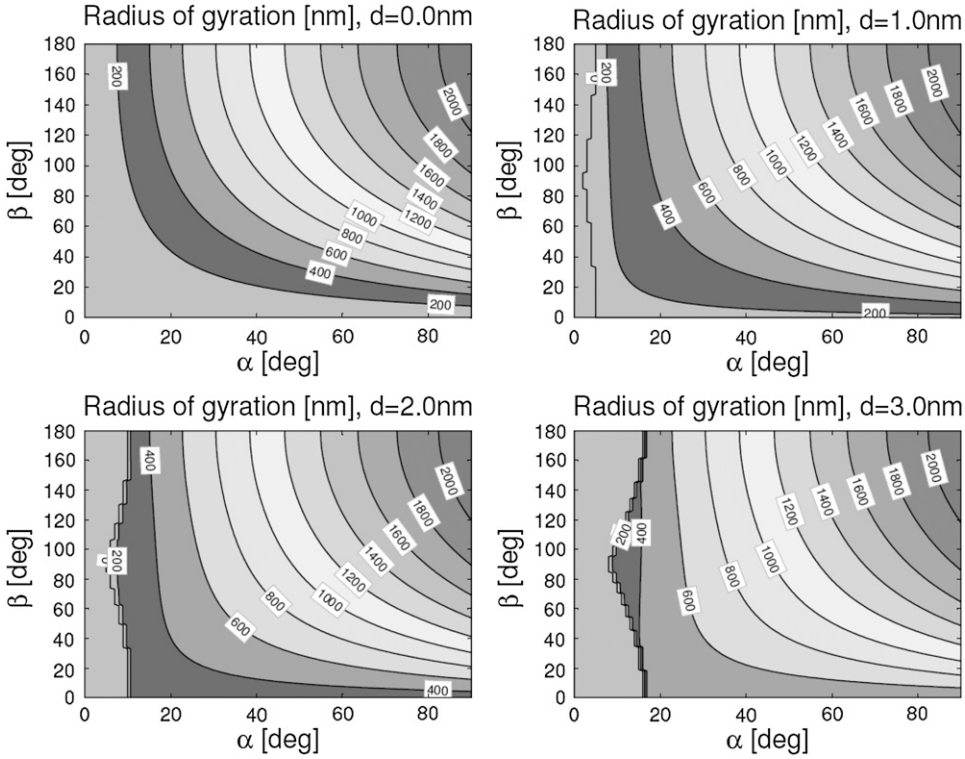


FIGURE 6 The radius of gyration of regular chromatin fibers along a cutout of the phase diagram with fixed fiber length of $N = 500$ segments. The compaction of the fibers decreases strongly with increasing $d$.

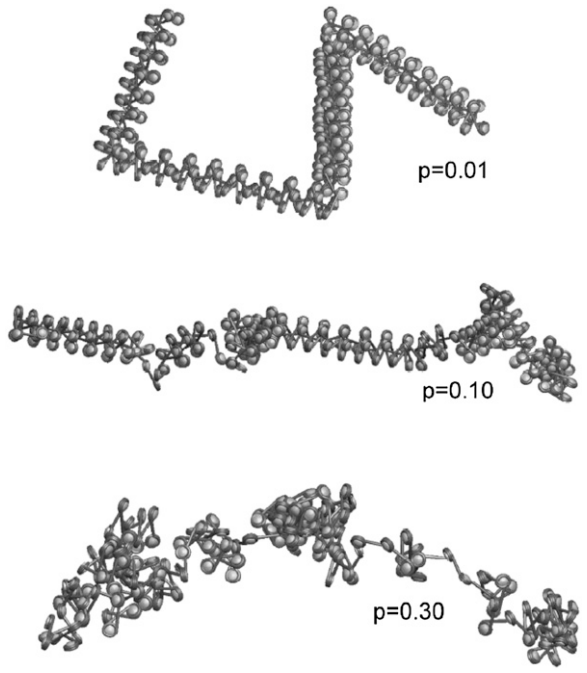


FIGURE 7 Chromatin fibers with different defect probabilities $p$. At $p = 0.30$ the regular structure of the 30-nm strand is almost completely collapsed.

somes, leading to a larger variety of allowed rotational angles $\beta$ and thus to the missing tip at the top of the peaks. This effect gets weaker with increasing $d$: The edges that cut the peaks become more parallel to the $\alpha$-axis.

With increasing orthogonal distance between in and outgoing DNA strand there is also more space between consecutive nucleosomes, leading to a decrease of the borderline. More and more states become accessible, and with $h = 5.5$ $\langle$bp$\rangle$ the borderline almost vanishes. The natural mean value

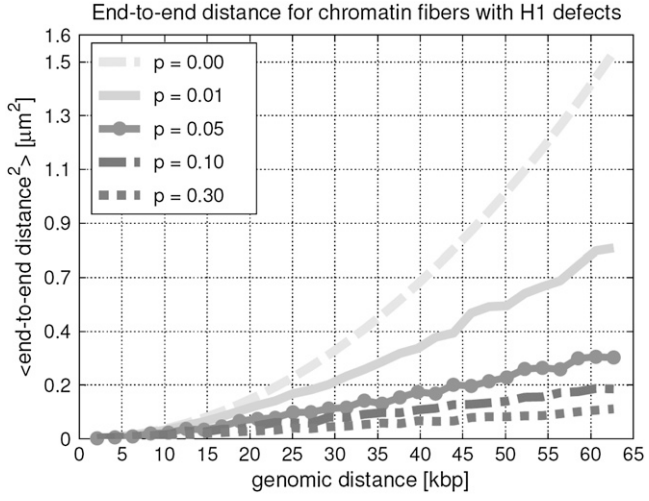


FIGURE 8 The mean end-to-end distance for chromatin fibers with H1 defects. With increasing defect probability $p$, the length of the fibers decreases rapidly. H1 defects might play a crucial role for chromatin compaction.

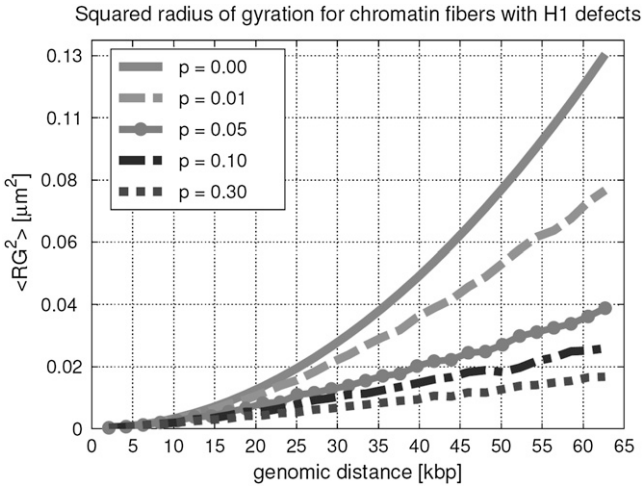


FIGURE 9 The squared radius of gyration for chromatin fibers with different defect probabilities $p$. With increasing number of H1 defects, the fiber becomes much more compact, which could be an important mechanism to compact the chromatin fiber.

of $h$ is $\sim h = 2.8$ nm $= 8.4$ $\langle$bp$\rangle$ due to 1.65 turns of DNA, with a diameter of 2.2 nm. Lower $h$ values might occur where the DNA has less turns around the histone complex.

We furthermore examined the line density (defined as the number of nucleosomes along an 11-nm stretch of the chromatin fiber; Fig. 5) and the radius of gyration (Fig. 6) of regular chromatin fibers (length 500 nucleosomes) along the phase diagram. The most compact states can be found near the excluded volume borderline. The line densities we found in our simulations coincide with experimental values (30). Increasing $d$ decreases the line density and increases the radius of gyration. The line densities at the peaks of the borderline are approximately twice the densities in the gaps (see Fig. 5).

## H1 defects

We also investigated the influence of missing H1 histones on the mean squared end-to-end distance (Figs. 7 and 8) and the mean squared radius of gyration (Fig. 9) of chromatin fibers. The parameter $p$ gives the defect probability in this section. One can clearly see that even very small defect rates of some percent have a huge effect on the compaction of chromatin: Both the mean squared radius of gyration and the mean end-to-end distance decrease rapidly if one allows only a few H1 defects. Without H1 defects ($p = 0$) we get an ideal chromatin fiber within the restriction of the extended two-angle model. This ideal fiber reflects the properties of the 30-nm strand only on small length scales. Therefore, the increase of the compaction due to defects will probably be not as strong, as implicated by our results. Nevertheless, missing H1 histones might contribute to chromatin compaction and DNA accessibility for transcription purposes at the same time, since one can see from Fig. 7 that although the fiber gets more compact,

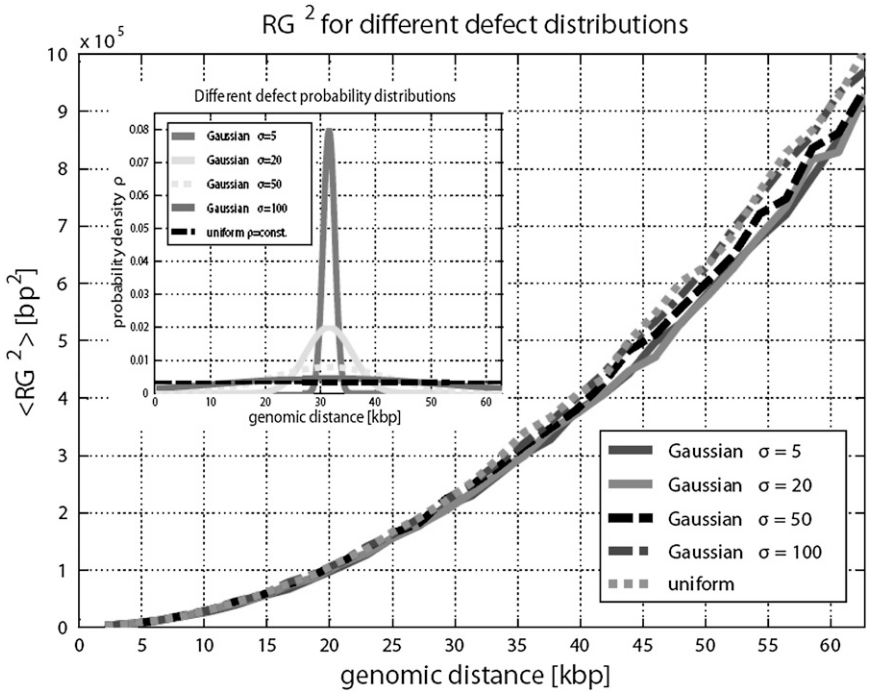


FIGURE 10 The squared radius of gyration for different defect probability distributions $\rho$ and different fiber lengths. The probability density function range, from a Gaussian peak in the middle of the chromatin fiber, to a uniform defect probability distribution along the whole fiber. The corresponding squared radius of gyration is quite independent of the defect distribution.

some very open parts appear. One can also see here the increasing disorder with increasing $p$. Fig. 7 shows visual similarities with EC-M images (for instance, Figs. 1 and 2 in (7)) that show typical chromatin confirmations. This might, among others, come from H1 defects in the fiber.

Fig. 10 shows the behavior of the squared radius of gyration in dependence of the fiber length for different defect probability distributions. The probability density functions range from a Gaussian peak in the middle of the fiber to a uniform probability density function along the whole chromatin strand (see Fig. 10, *inset*). Nevertheless, the effect on the squared radius of gyration is small.

## DISCUSSION

The compaction of chromatin is still an open question. A polymer of a total length of two meters has to fit into a tiny cell nucleus of some microns. We showed two possible strategies for the fiber to deal with this task. The fiber might use gaps in the phase diagram, i.e., very dense states to compact parts of itself. To do so core histone modifications or changes of the entry-exit angle by changes of the salt concentration might play a role. Furthermore, we showed that missing H1 histones might supply a further contribution to the compaction of the fiber. These H1 defects might play a crucial role in the task of chromatin compaction and at the same time serve the transcription of the DNA by opening locally the chromatin fiber. Taking fluctuations of the basic model parameters into account, the end-to-end distance and the radius of gyration will not decrease that strongly any more with increasing defect probability. But nevertheless, we think that H1 defects play a role in chromatin compaction.

Moreover, we developed the ordinary two-angle model further to our E2A model, which is much more detailed and thus appropriate to model chromatin at the 30-nm level.

We thank Giacomo Cavalli, Jörg Langowski, and Roel van Driel for fruitful discussions.

## REFERENCES

1. van Holde, K. E. 1989. Chromatin. Springer-Verlag, New York.
2. Davey, C. A., D. F. Sargent, K. Luger, A. W. Maeder, and T. J. Richmond. 2002. Solvent mediated interactions in the structure of the nucleosome core particle at 1.9 Å resolution. *J. Mol. Biol.* 319:1097–1113.
3. Luger, K., A. W. Mader, R. K. Richmond, D. F. Sargent, and T. J. Richmond. 1997. Crystal structure of the nucleosome core particle at 2.8 Ångstrom resolution. *Nature.* 389:251–260.
4. Fan, Y., T. Nikitina, J. Zhao, T. S. Fleury, R. Bhattacharyya, E. E. Bouhassira, A. Stein, C. L. Woodcock, and A. I. Skoultchi. 2005. Histone H1 depletion in mammals alters global chromatin structure but causes specific changes in gene regulation. *Cell.* DOI 110.1016/J.2005.10.028.
5. Lia, G., E. Praly, H. Ferreira, C. Stockdale, Y. C. Tse-Dinh, D. Dunlap, V. Croquette, D. Bensimon, and T. Owen-Hughes. 2006. Direct observation of DNA distortion by the RSC complex. *Mol. Cell.* 21:417–425.
6. Thoma, F., Th. Koller, and A. Klug. 1979. Involvement of histone H1 in the organization of the nucleosome and of the salt-dependent superstructures of chromatin. *J. Cell Biol.* 83:403–427.
7. Bednar, J., R. A. Horowitz, S. A. Grigoryev, L. M. Carruthers, J. C. Hansen, A. J. Koster, and C. L. Woodcock. 1998. Nucleosomes, linker DNA, and linker histone form a unique structural motif that directs the higher-order folding and compaction of chromatin. *Proc. Natl. Acad. Sci. USA.* 95:14173–14178.
8. Widom, J. 1986. Physicochemical studies of the folding of the nucleosome filament into the filament. Cation dependence. *J. Mol. Biol.* 190:411–424.

9. Chakravarthy, S., Y. J. Park, J. Chodaparambil, R. S. Edayathumangalam, and K. Luger. 2005. Structure and dynamic properties of nucleosome core particles. *FEBS Lett*. 579:895–898.

10. Holde, K. V., and J. Zlatanova. 1995. Chromatin higher order structure: chasing a mirage? *J. Biol. Chem*. 270:8373–8376.

11. Holde, K. V., and J. Zlatanova. 1996. What determines the folding of the chromatin fiber? *Proc. Natl. Acad. Sci. USA*. 93:10548–10555.

12. Schalch, T., S. Duda, D. F. Sargent, and T. J. Richmond. 2005. X-ray structure of a tetranucleosome and its implications for the chromatin fiber. *Nature*. 436:138–141.

13. Woodcock, C. L., S. A. Grigoryev, R. A. Horowitz, and N. Whitaker. 1993. A chromatin folding model that incorporates linker variability generates fibers resembling the native structures. *Proc. Natl. Acad. Sci. USA*. 90:9021–9025.

14. Schiessel, H., W. M. Gelbart, and R. Bruinsma. 2001. DNA folding: structural and mechanical properties of the two-angle model for chromatin. *Biophys. J*. 80:1940–1956.

15. Dorigo, B., T. Schalch, A. Kulangara, S. Duda, R. R. Schroeder, and T. J. Richmond. 2004. Nucleosome arrays reveal the two-start organization of the chromatin fiber. *Science*. 306:1571–1573.

16. Finch, J. T., and A. Klug. 1976. Solenoidal model for superstructure in chromatin. *Proc. Natl. Acad. Sci. USA*. 73:1897–1901.

17. Widom, J., and A. Klug. 1985. Structure of the chromatin filament: x-ray diffraction from oriented samples. *Cell*. 43:207–213.

18. Odenheimer, J., G. Kreth, and D. W. Heermann. 2005. Dynamic simulation of active/inactive chromatin domains. *J. Biol. Phys*. 31: 351–363.

19. Bednar, J., R. A. Horowitz, J. Dubochet, and C. L. Woodcock. 1995. Chromatin conformation and salt-induced compaction: three dimensional structural information from cryoelectron microscopy. *J. Cell Biol*. 131:1365–1376.

20. Zlatanova, J., S. H. Leuba, and K. van Holde. 1998. Chromatin fiber structure: morphology, molecular determinants, structural transitions. *Biophys. J*. 74:2554–2566.

21. Leuba, S. H., G. Yang, C. Robert, B. Samori, K. van Holde, J. Zlatanova, and C. Bustamante. 1994. Three-dimensional structure of extended chromatin fibers as revealed by tapping-mode scanning force microscopy. *Proc. Natl. Acad. Sci. USA*. 91:11621–11625.

22. Gerchman, S. E., and V. Ramakrishhnan. 1987. Chromatin higher-order structure studied by neutron scattering and scanning transmission electron microscopy. *Proc. Natl. Acad. Sci. USA*. 84:7802–7806.

23. Mergell, B., R. Everaers, and H. Schiessel. 2004. Nucleosome interactions in chromatin: fiber stiffening and hairpin formation. *Phys. Rev. E*. 70:011915-1–011915-9.

24. Barbi, M., J. Mozziconacci, and J. M. Victor. 2004. How the chromatin fiber deals with topological constraints. *Phys. Rev. E Stat. Nonlin. Soft Matter Phys*. 71:031910.

25. Schiessel, H. 2003. Topical review: the physics of chromatin. *J. Phys. Condens. Matter*. 15:R699–R774.

26. Diesinger, P. M., and D. W. Heermann. 2006. Two-angle model and phase diagram for chromatin. *Phys. Rev. E Stat. Nonlin. Soft Matter Phys*. 74:031904.

27. Binder, K., and D. W. Heermann. 2002. The Monte Carlo Method in Statistical Physics, 4th Ed. Springer Series in Solid-State Sciences, New York.

28. Wolffe, A. 1999. Chromatin: Structure and Function, 3rd Ed. Academic Press, New York.

29. de Gennes, P. G. 1979. Scaling Concepts in Polymer Physics. Cornell University Press, Ithaca, NY.

30. Bystricky, K., P. Heun, L. Gehlen, J. Langowski, and S. M. Gasser. 2004. Long-range compaction and flexibility of interphase chromatin in budding yeast analyzed by high-resolution imaging techniques. *Proc. Natl. Acad. Sci. USA*. 101:495–500.